Journal of Photochemistry & Photobiology, A: Chemistry 449 (2024) 115371

Contents lists available at ScienceDirect

Journal of Photochemistry & Photobiology, A: Chemistry

journal homepage: www.elsevier.com/locate/jphotochem

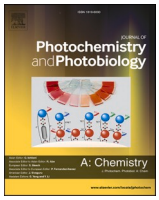

Ultraviolet absorption spectra of acrylic acid and its conjugate base, acrylate, in aqueous solution

Lei Xue, David J. Kieber *

Department of Chemistry, State University of New York, College of Environmental Science and Forestry, 1 Forestry Drive, Syracuse, NY 13210, United States

ARTICLE INFO

Keywords:
Carboxylic acid
Molar absorptivity
Propionate
Dimethylsulphoniopropionate
Isosbestic point
Marine

ABSTRACT

Acrylic acid is an important compound widely used in industry with multiple commercial applications, and it is also a key intermediate in the marine organosulfur cycle. However, the fundamental ultraviolet (UV) absorption spectrum of acrylic acid or its conjugate base, acrylate ($pK_a = 4.25$ at 20 °C) have not been determined in water. In this paper, we determined the absorption spectrum of acrylate in aqueous solution at pH 7.2 and 20 °C between 207 and 400 nm. The molar absorptivity decreased rapidly from 3958 M^{-1} cm^{-1} at 207 nm to a non-detectable value at wavelengths greater than 330 nm, with weak absorption at wavelengths greater than 290 nm (e.g., ε_{290nm} 2.7 M^{-1} cm^{-1}). No discernable absorption bands were observed in the absorption spectrum. Excellent agreement was observed when comparing absorption spectra obtained (1) with two different spectrophotometers and (2) with standards prepared from either newly purchased sodium acrylate or from acrylate obtained from the base hydrolysis of dimethylsulfoniopropionate. Wavelength-dependent molar absorptivities were constant at pH 7.2 over a range of acrylate concentrations from 25 to 135 μM. The absorption spectrum red shifted when the solution pH increased from 2.8 to 8.2, with an isosbestic point observed at 214 nm indicating two exchangeable species in solution. Our study provides the first detailed UV absorption spectra of acrylic acid and acrylate in aqueous solution, with important implications regarding the detection and study of these compounds in environmental settings and commercial applications.

1. Introduction

Acrylic acid and its conjugate base, acrylate, undergo numerous reactions with free radicals, electrophilic or nucleophilic agents, and they also polymerize easily in the presence of acids, alkalis, amines, iron salts, peroxides, or light [1]. As a result, acrylic acid is used extensively in industry as an additive, chemical intermediate, and polymerizing agent. Acrylic acid is produced on a large scale globally (3.8×10^9 kg annually [2]) as an industrial raw material in the manufacture of a myriad of products including, for example, surface coatings, textiles, adhesives, paper coatings, polishes, paint formulations, cosmetics, and super absorbent materials such as diapers [3,4].

In addition to its industrial and commercial applications, acrylic acid is ubiquitous in the biosphere. Acrylic acid has been detected in many species of marine macro and micro algae [5–10], shallow-water corals [11–13], banana pulp extract [14], oysters [15], scallops [16], bacteria [17–20], the stomach of sheep [21], the digestive tract of penguins [22], and fish [23]. Acrylic acid has also been detected in the atmosphere [24] and in seawater [25–28].

The main natural precursor of acrylic acid is dimethylsulfoniopropionate (DMSP), a sulfur-containing secondary metabolite produced by many marine algae including coccolithophores, dinoflagellates and diatoms, macroalgae, and a few sea angiosperms [29]. The enzymatic cleavage of DMSP, a process generally mediated by DMSP lyases, leads to the production of acrylic acid and dimethylsulfide [30]. It is unclear why marine algae produce acrylic acid since it is a well-known toxin in cellular systems [19,20]. Nonetheless, several physiological and ecological functions have been proposed. Acrylate is proposed to serve as an antibiotic [5,31,32], a chemical defense against grazing [33] or viral attack [9], an antioxidant [10,34], a carbon overflow molecule [10,35], a structural support in mucous membranes [7], and a carbon substrate for microbial growth [27,36–39]. In the cell, acrylate may be transformed to 3-hydroxypropionate [17,40] via a CoA transferase and a hydratase, followed by further metabolism by an alcohol dehydrogenase to malonate semialdehyde and to acyl CoA plus CO_2 via aldehyde dehydrogenase [18].

Acrylic acid is very reactive due to an α-β double bond, which is why acrylic acid is used extensively as a polymerizing agent in industrial

* Corresponding author.
E-mail address: djkieber@esf.edu (D.J. Kieber).

https://doi.org/10.1016/j.jphotochem.2023.115371
Received 18 July 2023; Received in revised form 16 October 2023; Accepted 26 November 2023
Available online 28 November 2023

applications. In the presence of heat, acrylic acid can easily undergo free radical polymerization through a thermodynamically controlled addition reaction to form dimers [41]. Because acrylic acid is so reactive, vigorous polymerization and explosive accidents can occur from accidental overheating even when a radical inhibitor is added to storage tanks [42].

The dissociation of gas-phase acrylic acid is initiated by the absorption of ultraviolet radiation, resulting in decarboxylation and decarbonylation [43,44]. Likewise, aqueous solutions of acrylic acid undergo decarboxylation following absorption of radiation in the far UV (ca. 193 nm), which is a well-known photochemical degradation pathway in water and organic solvents for not only acrylic acid but more generally aliphatic carboxylic acids and compounds containing the carboxyl moiety (for review see [45]).

Compared to aliphatic carboxylic acids that do not contain the α-β double bond, the absorption of acrylic acid is significantly red-shifted owing to the resonance delocalization of the π electrons between the carbon–carbon double bond and the carboxyl group. However, a full UV absorption spectrum of acrylic acid or acrylate in water is currently lacking in the literature. Ref [46] reported only an absorption maximum of 15,000 M^{-1} cm^{-1} for acrylic acid in water at 194.4 nm, and no trend was observed with changes in the solvent polarity and the $\pi \rightarrow \pi^*$ transition energy for acrylic acid. Lüthy [47] determined the absorption spectrum of acrylic acid in hexane and found that the molar absorptivity decreased rapidly with increasing wavelength from ~32,000 M^{-1} cm^{-1} at 207 nm to 1 M^{-1} cm^{-1} at 283 nm with no observable absorption bands. A weak absorption peak was observed at ~250 nm for acrylic acid in cyclohexane [48]. However, this peak and the absorption spectrum varied as a function of acrylic acid concentration between 0.89 and 260 mM indicating that polymeric forms of acrylic acid affected the absorption spectrum (e.g., dimers [48]).

Given the importance of acrylic acid in nature and in industrial, commercial and research applications, it is surprising how little is known regarding the fundamental absorption properties of acrylic acid in aqueous solution. Therefore, in the present study, we determined the absorption spectrum of acrylic acid in high-purity water as a function of concentration and pH. This study is now possible because of the development of long-pathlength spectrophotometry. The absorption spectrum of an analyte can now be determined at low analyte concentrations using a long pathlength cell (e.g., 1 m) thereby minimizing potential secondary reactions or interactions that may affect the absorption spectrum of the analyte at higher concentrations. This is especially important for acrylic acid since it easily polymerizes and can undergo extensive hydrogen bonding.

2. Material and methods

2.1. Chemicals and reagents

Sodium acrylate (≥97 %) and acidimetric standard-grade potassium hydrogen-phthalate (99.95–100.05 %) were purchased from Sigma-Aldrich. DMSP hydrochloride was purchased from Research Plus Corporation. Propionic acid (>99 %) was received from VWR International. Sodium hydroxide pellets (≥97 %) were obtained from Alfa Aesar. Ultrapure hydrochloric acid was purchased from BDH. Standard reference potassium dichromate was obtained from EMD and phenol red sodium salt (ACS grade) was obtained from VWR. Tris (hydroxymethyl) aminomethane (≥99.9 %) and perchloric acid (ACS grade) were purchased from Sigma-Aldrich. Sodium bicarbonate (USP grade), and monobasic and dibasic sodium phosphate (99.9 %) were purchased from J. T. Baker. Methanol (≥99.9 %) was obtained from Burdick & Jackson. The high purity laboratory water used throughout this study, with resistivity of >18.2 MΩ-cm, was obtained from a Milli Q® gradient A10 ultrapure water system (EMD Millipore, Billerica, MA); hereafter this water is referred to as Milli-Q water.

2.2. Acrylic acid standard preparation and purity

Sodium acrylate degraded during short-term storage at room temperature in a desiccator (section 2.5). Therefore, the acrylate stock solution was routinely prepared from newly purchased, recently manufactured sodium acrylate. Additionally, standards prepared from sodium acrylate were periodically compared to acrylate standards prepared from the alkaline hydrolysis of an aqueous solution of DMSP to determine if the sodium acrylate degraded. To prepare an acrylate primary standard from DMSP, 1 mL of a 10 M NaOH solution was added to 10 mL of a 2 mM DMSP standard in a 30 mL borosilicate serum vial that was crimped-sealed with an aluminum cap containing a Teflon-faced butyl rubber stopper. Under basic conditions and at room temperature, the DMSP is quantitatively converted to dimethylsulfide (DMS) and acrylic acid [49]. The basified standard was incubated overnight at room temperature and subsequently bubbled for 30 min with ultrapure He to remove DMS followed by pH neutralization using ultrapure HCl (12 M). Except where noted, aliquots of the 2 mM primary standard prepared from either sodium acrylate or DMSP were diluted in pH 7.2, 5 mM bicarbonate buffer to produce secondary standards used for spectrophotometric studies. The primary acrylate standards were kept frozen at $^{-}20$ °C when not in use.

The purity of the sodium acrylate and DMSP was determined by comparing the carbon content in a series of acrylate or DMSP standards prepared in Milli-Q water to the carbon content predicted from the mass of acrylate or DMSP used to prepare the standards. The carbon content of the aqueous standards was quantified with a Model TOC-VCSH Shimadzu total organic carbon (TOC) analyzer. The TOC analyzer converted the organic carbon to CO_2 by sample combustion at 670 °C in a packed quartz column containing quartz beads and a catalyst, platinum balls; prior to sample injection into the TOC analyzer, samples were acidified and bubbled with zero air to remove dissolved inorganic carbon. The carbon measurements for acrylate or DMSP standards were calibrated against the primary standard, potassium hydrogen phthalate.

2.3. Absorbance measurements

A fiber optic spectrophotometer (model SD-2000, Ocean Optics) was used to determine absorption spectra between 240 and 800 nm. This spectrophotometer was equipped with a 101 cm liquid waveguide capillary cell (LWCC, World Precision Instruments). The cell pathlength was determined using phenol red and potassium dichromate as reference materials based on the procedure outlined in ref [50]. The incident radiation was provided by a combination of deuterium and tungsten halogen lamps (DH-2000) with a spectral output between 240 and 800 nm. The light sources and detector were allowed to stabilize for 2 h before recording absorption spectra. Since the lower wavelength limit of the Ocean Optics spectrophotometer is 240 nm, a model 8453 Hewlett Packard spectrophotometer was used to determine absorption spectra between 207 and 240 nm using a 5 cm-pathlength quartz cell. Except when noted, absorption spectra from two independent systems were merged to produce the absorption spectrum from 207 to 400 nm. Absorption spectra from both instruments were baseline corrected (see below) prior to merging. Typically, 3 to 5 replicate standards were analyzed using the Ocean Optics or Hewlett Packard spectrophotometer. The coefficient of variation among scans for replicate standards was small, ~1–2 % at all wavelengths, similar to the coefficient of variation of four repeated scans of the same standard.

The Ocean Optics 101 cm-pathlength cell was cleaned by alternate rinsing with spectrophotometric-grade MeOH and Milli-Q water. Except when noted, after rinsing the cell, a pH 7.2, 5 mM bicarbonate buffer was slowly drawn into the cell using a Rainin Rabbit-Plus peristaltic pump to obtain a reference spectrum. Absorption spectra were then recorded for several acrylate standards in pH 7.2, 5.0 mM bicarbonate buffer. Sample spectra were referenced against the absorption spectrum of the bicarbonate buffer and were corrected for baseline offsets.

Measurements were made at 20 ± 0.5 °C to minimize changes in the refractive index of water due to changes in temperature [51]. The wavelength-dependent absorbance, A_λ, was converted to the corresponding molar absorptivity, ε_λ (M^{-1} cm^{-1}), using Beer's law:

$$A_\lambda = \varepsilon_\lambda \cdot b \cdot C \quad (1)$$

where b (cm) is the cell pathlength, and C (M) is the concentration of the standard.

2.4. pH study and pK_a determination

The absorption spectrum of a 50 μM acrylic acid standard was determined at several pHs between 2.8 and 8.2 using the Hewlett Packard UV–Vis spectrophotometer. Buffers with different pHs were prepared using mixtures of 50 mM phosphoric acid, mono basic, and dibasic phosphate buffers. The pH for each buffer was determined using a Thermo-Scientific micro pH electrode coupled to an Orion 3 Star benchtop meter. To determine an absorption spectrum, the spectrophotometer was first referenced using the corresponding pH buffer solution. The acid dissociation constant (K_a) of acrylic acid was determined using absorbance data at different pHs and the method outlined in ref [52]. Briefly, the equation for the acid dissociation constant, K_a, relating the concentrations of acrylic acid [HA] and its conjugate base acrylate [A^-] as a function of [H^+], is given as:

$$K_a = \frac{[H^+][A^-]}{[HA]} \quad (2)$$

The corresponding equation for the wavelength-dependent molar absorptivity of the solution (ε) is:

$$\varepsilon = \frac{\varepsilon_{HA}[HA] + \varepsilon_{A^-}[A^-]}{[HA] + [A^-]} \quad (3)$$

where ε_{HA} and ε_{A^-} are the wavelength-dependent molar absorptivities of acrylic acid and acrylate, respectively. Combining equations (2) and (3) yields equation (4):

$$\varepsilon = \varepsilon_{HA} + K_a \frac{\varepsilon_{A^-} - \varepsilon}{[H^+]} \quad (4)$$

The molar absorptivities of acrylic acid and acrylate were determined from absorbance measurements made at low and high pH where only one species was present in solution. K_a was determined from the slope of ε plotted as a function of $\frac{\varepsilon_{A^-} - \varepsilon}{[H^+]}$. K_a was calculated at five wavelengths between 210 and 230 nm. Only absorbance data at pHs 2.8, 3.4, 4.0, and 5.2 were used to calculate ε in equation (4), since the difference $\varepsilon_{A^-} - \varepsilon$ was very close to zero at pHs substantially greater than the pK_a (e.g., 6.4) leading to large errors.

2.5. Sodium acrylate stability study

The stability of the Sigma-Aldrich sodium acrylate was determined by comparing acrylate standards prepared in 0.2 μm-filtered seawater collected from the Sargasso Sea using a six-month old sodium acrylate to the concentration of (1) standards prepared using newly purchased sodium acrylate or (2) standards prepared from acrylate obtained from the base hydrolysis of DMSP. For this comparison, the acrylate concentration in each standard was determined using high performance liquid chromatography (HPLC) with UV absorbance detection of the acrylate derivative at 257 nm. The acrylate was derivatized and quantified using a pre-column derivatization method based on the Michael Addition of thiosalicylic acid to the acrylate carbon–carbon double bond [27].

2.6. Acrylate and propionate absorption spectra

The absorption spectrum of a solution of the conjugate base of the carboxylic acid, propionate, was compared to that for acrylate to highlight the difference in absorption spectra due to acrylate's carbon–carbon double bond. Absorption spectra were determined for 50 μM solutions of acrylate and propionate ($pK_a = 4.88$) prepared in pH 8.2, 50 mM phosphate buffer using a model 8453 Hewlett Packard UV–Vis spectrophotometer and a 5 cm quartz cell. All absorption spectra were referenced against the spectrum of the pH 8.2, 50 mM phosphate buffer.

2.7. Statistical analyses

All statistical analyses, including simple linear regressions and two-tailed t-tests, were performed using SigmaPlot software (version 11.0, Systat Software). Unless noted, an α level of 0.05 was used for all tests.

3. Results and discussion

3.1. Calibration and purity

Aqueous standards prepared from a six-month old sodium acrylate had HPLC responses that were 52 % lower compared to aqueous standards prepared from newly purchased sodium acrylate or standards prepared from acrylate obtained by the base hydrolysis of DMSP (Fig. 1). Standard regression slopes (±std dev) were 59.1 (±1.7), 119.5 (±2.3) and 117.0 (±0.6) nM^{-1}, respectively, for the old, new, and DMSP-derived acrylate standards. The slopes of the new acrylate and DMSP-derived acrylate standards were statistically indistinguishable based on a t test ($p > 0.05$), whereas the slope of the old acrylate standard was significantly lower than either the new acrylate or DMSP-derived acrylate standards ($p < 0.05$).

Acrylic acid was not used to prepare standards in the present study because a polymerization inhibitor is added to all commercial formulations, which would affect absorption spectra. The sodium acrylate salts did not contain a stabilizer. However, comparison of standard HPLC responses demonstrated that the sodium acrylate degraded when stored at room temperature in a desiccator as recommended by the manufacturer, and therefore care should be taken when using acrylate salts as standards.

Comparison between the measured carbon and predicted carbon in a series of DMSP or acrylate (new bottle) standards prepared in Milli-Q

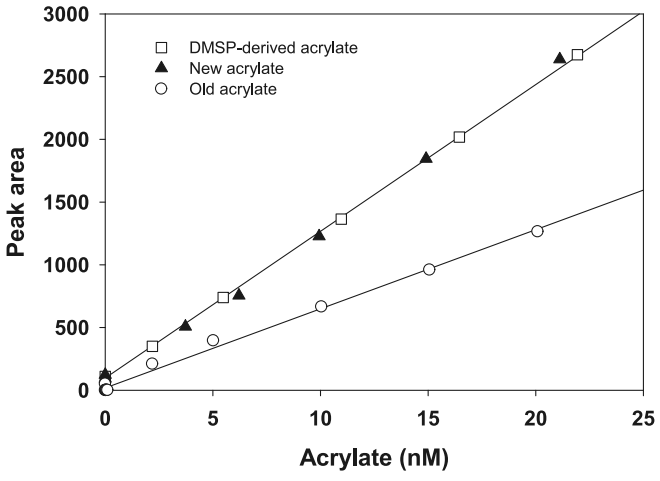

Fig. 1. Acrylate HPLC peak area plotted as a function of acrylate concentration. Acrylate standards were prepared from the hydrolysis of a DMSP standard (squares, slope ± std dev = 117.0 ± 0.6 nM^{-1}), from a newly purchased bottle of sodium acrylate (triangles, slope ± std dev = 119.5 ± 2.3 nM^{-1}) or from a six-month old bottle of sodium acrylate (circles, slope ± std dev = 59.1 ± 1.7 nM^{-1}). All standards were prepared by adding μL quantities of a 0.4 μM acrylate standard into 3 mL of 0.2 μm-filtered Sargasso Sea seawater. The concentration of acrylate in the seawater samples with no added acrylate was ~0.5 nM.

water are shown in Fig. 2. For acrylate, linear regression analysis between the measured and predicted carbon concentrations yielded a slope (±std dev) of 0.999 (±0.009). Likewise, excellent agreement was observed between the measured and predicted carbon for DMSP, with a slope (±std dev) of 0.988 (±0.009) based on linear regression analysis. Neither slope was significantly different from a slope of 1.0 based on a two-tailed *t*-test ($p < 0.0001$) confirming the purity of the chemicals within analytical uncertainty.

3.2. Absorption spectra

Short-chain α, β-unsaturated carboxylic acids including acrylic acid can undergo extensive hydrogen bonding and polymerize in polar and nonpolar solvents [46,48]. This is likely why there is virtually no information regarding the absorption spectrum of acrylic acid in aqueous solution in the literature. With the development of long pathlength spectrophotometry, it is now possible to determine the absorption spectrum of reactive compounds such as acrylic acid at relatively low concentrations thereby minimizing potential problems associated with solute–solute interactions and reactions observed at higher concentrations.

Absorption spectra of acrylate standards in 5 mM, pH 7.2 bicarbonate buffer were determined between 240 and 330 nm at concentrations ranging from 25 to 135 μM (Fig. 3, panel A). Each absorption spectrum was characterized by a rapid decrease in absorbance with increasing wavelength, with no absorption peaks or shoulders observed within this spectral range. Excellent linearity was observed when the absorbance at selected wavelengths was plotted as a function of acrylate concentration (Fig. 3, panel B). The lone exception to this finding was the nonlinearity observed at the shortest wavelength (250 nm) and the highest acrylate concentrations (Fig. 3, panel B), with corresponding absorbances that were greater than 1 and outside the range of linearity of the spectrophotometer. Linear absorbance dependencies with increasing acrylate concentrations indicated that concentration dependent solute–solute interactions such as H-bonding or reactions including dimerization and further polymerization were not important.

A study was conducted to compare the wavelength-dependent molar absorptivity of a 50 μM acrylate standard in a 5 mM, pH 7.2 bicarbonate buffer determined using the Ocean Optics spectrophotometer (101 cm pathlength flow cell) to that obtained using the model 8453 UV–Vis Hewlett Packard diode array spectrophotometer (5 cm pathlength quartz cell). When the spectra were plotted together, they overlapped with excellent agreement at a 95 % confidence interval (Fig. 4).

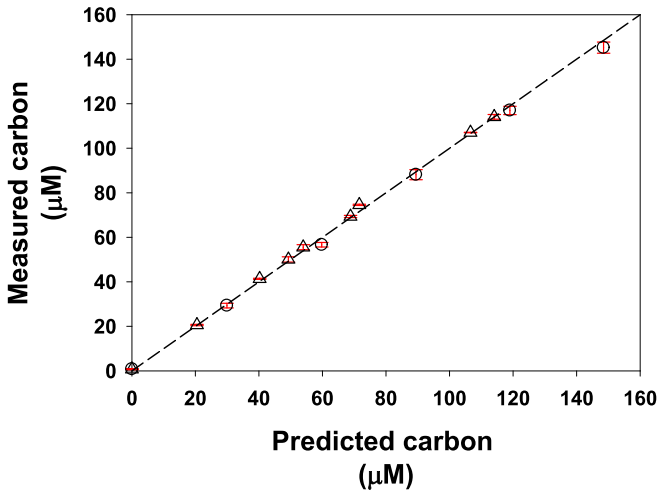

Fig. 2. Carbon concentration measured in acrylate (triangles) or DMSP (circles) aqueous standards using a Shimadzu model TOC-VCSH total organic carbon analyzer plotted against the carbon concentration predicted based on the weight of each standard. The dashed line represents the 1:1 ratio between measured and predicted carbon. Red vertical error bars denote the standard deviation from replicate carbon measurements (n = 3).

Since acrylate absorbances obtained by the two instruments were in excellent agreement, a composite wavelength-dependent molar absorptivity spectrum for acrylate was generated (Fig. 5) using absorbance data obtained with the Hewlett Packard spectrophotometer at wavelengths less 240 nm and the Ocean Optics spectrophotometer at wavelengths equal to and greater than 240 nm. The resultant wavelength-dependent molar absorptivity spectrum decreased rapidly from 3958 M^{-1} cm^{-1} at 207 nm to below detection at wavelengths greater than 330 nm (Fig. 5, Table 1).

Compared to its saturated analog, propionate, which showed no absorption beyond ~ 235 nm (Fig. 5, Table S1), acrylate absorbed UV much stronger at all wavelengths (e.g., 2784 vs 70 M^{-1} cm^{-1} at 210 nm), and the UV absorption spectrum of acrylate extended into the UV-B waveband (290⁻320 nm), demonstrating the impact of π electron delocalization between the α, β double bond and the carboxyl group on the absorption spectrum for acrylate compared to that for simple aliphatic acids such as propionate. Based on acrylate's absorption spectrum, it is worth noting that, unlike saturated carboxylic acids such as formic, acetic [53], or propionic acid (Fig. 5), acrylate weakly absorbs electromagnetic solar radiation in the spectral range that is relevant to aquatic photochemistry (≥ ~ 290 nm) in marine and freshwater systems, suggesting that acrylate can potentially undergo primary photolysis in sunlit surface waters. However, no photolysis was observed when a ~20 nM acrylate standard in Milli-Q water or seawater was exposed to irradiation from a solar simulator for several hours, indicating that the quantum yield for the primary photolysis of acrylate was too low [54].

Since solid sodium acrylate degraded after storage in the dark at room temperature, we also determined the absorption spectra of acrylate standards prepared using acrylate produced from the alkaline hydrolysis of DMSP. Absorbance spectra determined using the DMSP-derived standards were compared to absorbance spectra obtained using standards prepared from a new bottle of sodium acrylate. As with the HPLC comparison study, excellent agreement was observed between results obtained with the two different acrylate standards. The absorbance determined at a given wavelength (e.g., 250 nm) plotted as a function of acrylate concentration determined using the two different acrylate standards overlapped (Fig. 6, Table S2). This finding demonstrated that DMSP base hydrolysis can serve as a reliable method to prepare acrylate standards, which is advantageous since DMSP is stable in acidic solution [49] and can serve as a ready source of acrylate.

The UV absorption spectrum has not been previously documented for acrylic acid or acrylate in aqueous solution. The only absorption measurement made in water reported a molar absorptivity of 15,000 M^{-1} cm^{-1} at 194.4 nm for a 1 mM solution of acrylic acid at pH ~ 3.6 [46]. In all other studies, the absorption spectrum of acrylic acid was determined in organic solvents including hexane [47] and cyclohexane [48] using mM concentrations of freshly distilled acrylic acid. There was a large discrepancy in the molar absorptivities obtained in hexane [47] and in cyclohexane [48] despite the very similar polarities of these two nonpolar solvents (Fig. 7). Differences may have resulted from concentration-dependent variations in the degree of polymerization or H-bonding in these two studies. Given these differences, a detailed study is warranted to determine the impact of solvent polarity on the UV absorption of acrylic acid or acrylate at lower μM concentrations.

It is not possible to directly compare our absorption spectra determined in aqueous solution with published spectra [47,48] given the very different conditions and the lack of critical experimental information in these previous studies. Nonetheless, the effect of solvent polarity on absorption spectra can be examined qualitatively. An increase in the solvent polarity generally causes a blue shift in the $n \rightarrow \pi^*$ transition and a red shift in the $\pi \rightarrow \pi^*$ transition [55]. Our results are consistent with this trend. As shown in Fig. 7, our molar absorptivities determined in water were significantly higher at wavelengths greater than ~ 260 nm and substantially lower at wavelengths less than 215 nm compared to

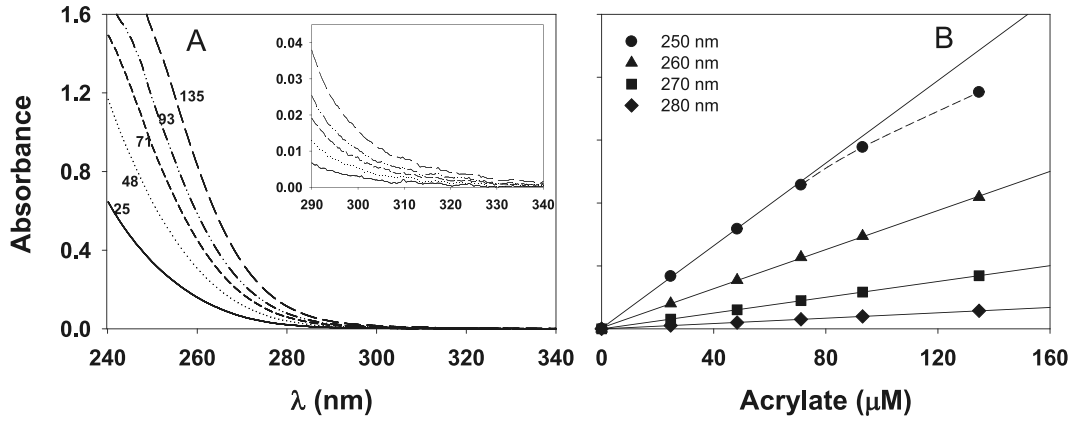

Fig. 3. (A) Absorption spectrum plotted as a function of acrylate concentration (25, 48, 71, 93, and 135 μM). Acrylate standards were prepared in 5 mM, pH 7.2 bicarbonate buffer. Spectra were determined at 20 °C using the Ocean Optics spectrophotometer with a 101 cm pathlength flow cell. The inset in panel A depicts concentration-dependent absorption spectra between 290 and 340 nm. (B) The absorbance at 250, 260, 270, and 280 nm plotted as a function of acrylate concentration.

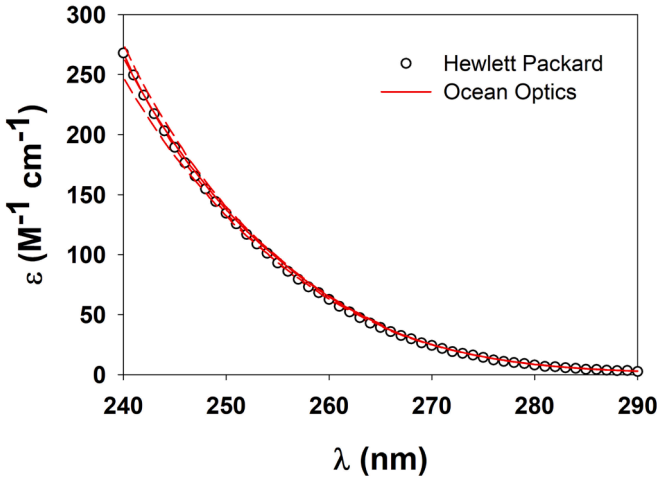

Fig 4. Wavelength-dependent molar absorptivity (ε) of a 50 μM acrylate solution in a 5 mM bicarbonate buffer at pH 7.2 between 240 and 290 nm determined using the model SD-2000 Ocean Optics spectrophotometer (101 cm pathlength cell, red solid line) and the 8453 Hewlett Packard spectrophotometer (5 cm pathlength cell, white-filled circles). The red dashed lines denote the upper and lower 95 % confidence interval for the absorption spectrum determined using the Ocean Optics spectrophotometer.

published molar absorptivities in the nonpolar solvent, hexane [47]. This trend suggests there was a blue shift at shorter wavelengths for the π → π* transition and a red shift at longer wavelengths for the n → π* transition when going from hexane to water.

A low-intensity absorption band corresponding to an n → π* transition may be expected for acrylic acid due to the non-bonding electrons on the carboxyl moiety. A 0.89 mM solution of acrylic acid in cyclohexane had a weak absorption band near 250 nm (ε, 600 M^{-1} cm^{-1}) that was ascribed to an n → π* transition [48]. A weak but distinct band was observed at 245 nm for dimethylacrylic acid in the gas phase at 70 °C; this band was suggested to correspond to the weak absorption of the n → π* transition for this α, β-unsaturated carboxylic acid [56]. A similar finding was observed for the ethyl ester of acrylic acid in the nonpolar solvent isooctane. This ester exhibited a distinct absorption maximum at 243 nm (ε, 70 M^{-1} cm^{-1}) in isooctane that was slightly blue shifted to 239 nm and less distinct in ethanol and completely missing in water [57]. A weak n → π* absorption band was not observed in our study or in six different solvents including water [46]. The disappearance of a distinct n → π* band might be explained by a blue shift of the absorption spectrum in water, a highly polar solvent, and the subsequent masking by the much larger absorption arising from the π → π* transition. For the n → π* transition, highly polar solvents such as water or methanol hydrogen bond to the ground state stronger than to the excited state. Consequently, the energy of the ground state is lowered more than that of the excited state, resulting in a larger energy requirement for the transition and subsequently a blue shift [55,58].

3.3. pH effect on absorption

The absorption spectrum of a 50 μM acrylate solution in 5 mM phosphate buffer changed as a function of the solution pH (Fig. 8, Table S3). The absorbance increased at wavelengths longer than 214 nm as the solution pH increased from 2.8 to 8.2, with the opposite trend observed at wavelengths less than 214 nm. The observed increase at wavelengths longer than 214 nm with increasing solution pH resulted from an increase in the acrylate concentration with increasing pH. The acrylate ion, and more generally the carboxylate ion, has a greater degree of electron delocalization on the carboxyl moiety compared to its conjugate acid, and a corresponding lower energy gap between molecular orbitals for electronic transitions [55] resulting in an increase in absorption. A similar pH effect was observed for the absorption of amino acids [59–61]), domoic acid [62], and a series of low molecular-weight carboxylic acids [63].

The absorption spectra at different solution pHs intersected at 214 nm, indicating the existence of an isosbestic point and demonstrating that there were two principal interchangeable species in solution, acrylic acid and its conjugate base, acrylate, that were responsible for the total absorbance. This isosbestic point provided further evidence that dimerization was not important in the absorbance of μM acrylate solutions. Using the molar absorptivity data at different pHs and the approach outlined in Ref [52], we determined that the pK_a (±std dev) of acrylic acid was 4.25 (±0.06) at 20 °C, which is in excellent agreement with the literature value of 4.25 at 25 °C in water [64]. The uncertainty of our pK_a estimate was determined by propagation errors associated with averaging the slopes from linear regression for data at individual wavelengths from 210 to 230 nm at 1 nm resolution (Fig. 9).

3.4. Acrylic acid and acrylate fluorescence

An experiment was conducted to determine if 5 mM buffered phosphate solutions of acrylic acid (pH 2.8) or acrylate (pH 8.2) fluorescenced at two concentrations, 50 and 100 μM. No fluorescence was observed for either compound at any emission wavelength when the excitation wavelength (±bandwidth) was set at 210, 230, 250, and 270

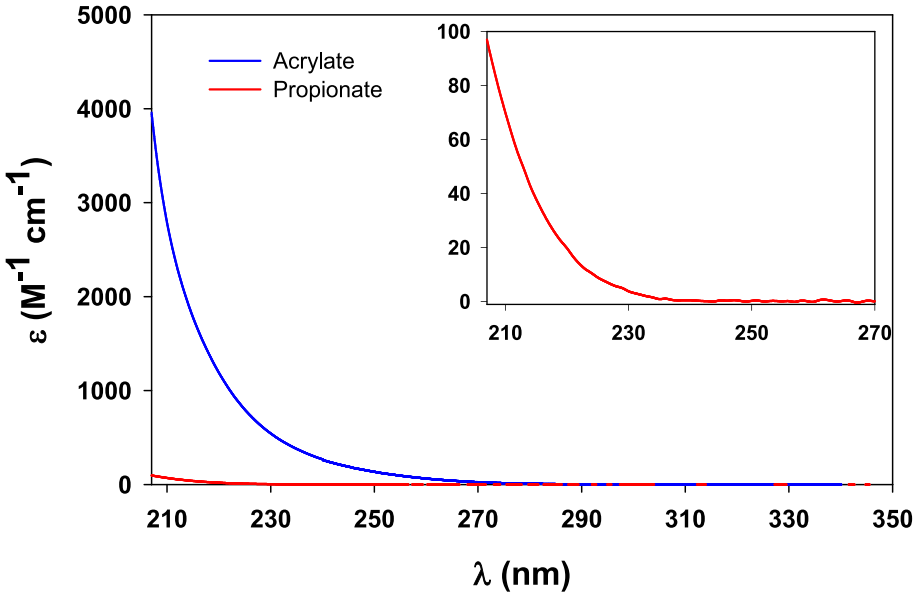

Fig 5. Molar absorptivity (ε) of acrylate (blue line) and propionate (red line) plotted as a function of wavelength (λ) from 207 to 350 nm. The inset depicts a re-scaled plot of ε for propionate from 207 to 270 nm. Absorbance measurements were made using 50 μM propionate and acrylate standards prepared in 5 mM, pH 8.2 phosphate buffers. All spectra were referenced against the 5 mM, pH 8.2 phosphate buffer. Data used to generate the absorption spectrum for propionate are presented in Table S1.

Table 1
The average (±std dev) molar absorptivity (M^{-1} cm^{-1}) of acrylate from 207 to 330 nm at 20 °C. Acrylate standards used for this study were prepared in a 5 mM, pH 7.2 bicarbonate buffer. The average molar absorptivity was determined at each wavelength by averaging the absorbance of five acrylate standards at concentrations between 25 and 135 μM.

λ (nm)	ε	λ (nm)	ε	λ (nm)	ε	λ (nm)	ε	λ (nm)	ε
207	3958 (59)	235	379 (5.7)	263	49.2 (0.7)	291	2.46 (0.07)	319	0.19 (0.05)
208	3486 (52)	236	354 (5.3)	264	44.9 (0.5)	292	2.20 (0.09)	320	0.17 (0.05)
209	3104 (47)	237	330 (4.9)	265	41.0 (0.4)	293	2.01 (0.07)	321	0.15 (0.03)
210	2784 (42)	238	308 (4.6)	266	37.4 (0.4)	294	1.83 (0.09)	322	0.14 (0.05)
211	2522 (38)	239	287 (4.3)	267	33.9 (0.3)	295	1.68 (0.09)	323	0.13 (0.04)
212	2298 (35)	240	268 (4.0)	268	30.8 (0.3)	296	1.55 (0.09)	324	0.12 (0.05)
213	2106 (32)	241	245 (4.2)	269	27.8 (0.3)	297	1.41 (0.09)	325	0.11 (0.01)
214	1934 (29)	242	230 (3.9)	270	25.2 (0.2)	298	1.29 (0.08)	326	0.10 (0.04)
215	1779 (27)	243	216 (3.7)	271	22.7 (0.2)	299	1.26 (0.08)	327	0.09 (0.04)
216	1642 (25)	244	203 (3.4)	272	20.5 (0.2)	300	1.16 (0.10)	328	0.08 (0.06)
217	1514 (23)	245	190 (6.4)	273	18.5 (0.2)	301	1.04 (0.08)	329	0.07 (0.04)
218	1399 (21)	246	176 (5.1)	274	16.6 (0.2)	302	0.94 (0.09)	330	0.07 (0.02)
219	1290 (19)	247	166 (4.3)	275	14.9 (0.2)	303	0.90 (0.11)		
220	1190 (18)	248	155 (3.8)	276	13.3 (0.1)	304	0.78 (0.08)		
221	1099 (17)	249	145 (3.5)	277	11.8 (0.1)	305	0.75 (0.09)		
222	1013 (15)	250	135 (3.1)	278	10.6 (0.1)	306	0.67 (0.11)		
223	934 (14)	251	125 (3.1)	279	9.45 (0.06)	307	0.59 (0.09)		
224	864 (13)	252	117 (2.4)	280	8.45 (0.08)	308	0.56 (0.09)		
225	798 (12)	253	109 (2.0)	281	7.59 (0.11)	309	0.49 (0.06)		
226	738 (11)	254	102 (1.8)	282	6.82 (0.10)	310	0.45 (0.08)		
227	683 (10)	255	94.3 (1.8)	283	6.03 (0.07)	311	0.41 (0.08)		
228	632 (10)	256	87.5 (1.5)	284	5.37 (0.12)	312	0.37 (0.07)		
229	586 (8.8)	257	81.1 (1.3)	285	4.73 (0.10)	313	0.34 (0.07)		
230	544 (8.2)	258	75.1 (1.1)	286	4.16 (0.11)	314	0.30 (0.05)		
231	505 (7.6)	259	69.0 (1.3)	287	3.71 (0.13)	315	0.28 (0.02)		
232	469 (7.0)	260	63.4 (1.1)	288	3.36 (0.08)	316	0.25 (0.04)		
233	437 (6.6)	261	58.4 (0.9)	289	3.05 (0.07)	317	0.23 (0.03)		
234	407 (6.1)	262	53.6 (0.7)	290	2.73 (0.09)	318	0.21 (0.06)		

(±8 nm) and the emission was scanned at wavelengths 15 nm greater than the excitation wavelength out to 500 nm at a wavelength resolution of 2 nm using an ISS model PC1 spectrofluorometer.

4. Conclusions

In this study we used LWCC-spectrophotometry to determine the absorption spectrum of a poorly absorbing, reactive compound in water, which had previously proven intractable. However, the value of LWCC methodology goes well beyond our study. This methodology is used in many fields of research including analytical chemistry, biochemistry, and environmental science. The increasing use of long pathlength spectroscopy is due to its enhanced sensitivity, improved limits of detection, and low sample volume requirement (ca. 250 μL) compared to standard benchtop spectroscopic techniques. LWCC cells are versatile and can be used in UV/Vis/NIR spectrophotometry, Raman and

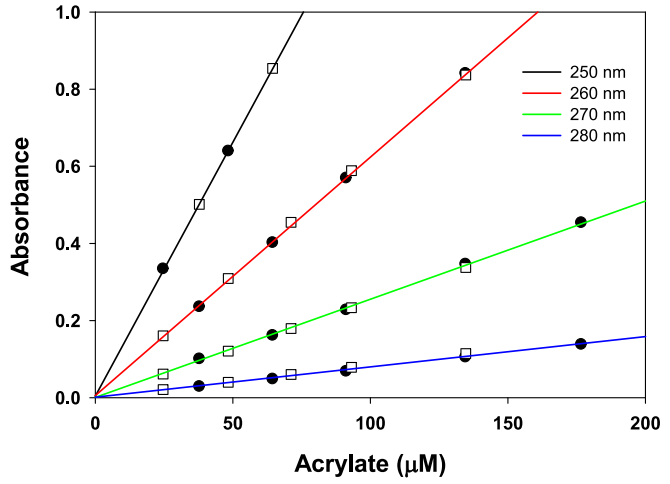

Fig 6. Absorbance of acrylate standards at 250, 260, 270, and 280 nm. Acrylate standards were prepared in pH 7.2, 5 mM bicarbonate buffer using either DMSP (black-filled circles) or newly purchased sodium acrylate (white-filled squares). All absorbance measurements were made using the Ocean Optics spectrophotometer with a 101 cm pathlength cell at 20 °C. The lines denote the best fits from linear regression analysis; data sets for standards prepared from sodium acrylate and DMSP were pooled for linear regression analysis at each wavelength. Data used in this figure are presented in Table S2.

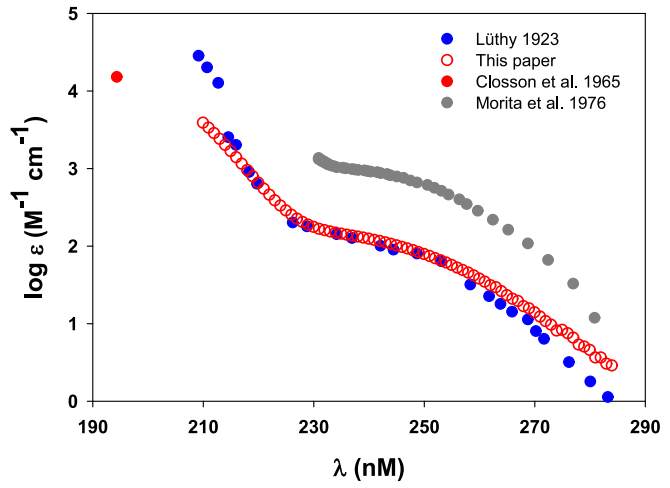

Fig. 7. Log scale of the molar absorptivity (ε) of acrylic acid determined in hexane (Lüthy 1923, blue-filled dots), cyclohexane (Morita et al. 1976, grey-filled dots), and in a 50 mM, pH 2.8 aqueous phosphate buffer (This study, red-edged circles). The solid red dot depicts the peak absorption observed at 194 nm for acrylic acid in water at pH 3.6 (Closson et al. 1965).

fluorescence spectroscopy, and in chemiluminescence systems to study the spectroscopic properties and quantify low concentrations of poorly absorbing and reactive chemical species. One field of study where long pathlength spectrophotometry finds widespread application is marine chemistry where LWCC spectrophotometers are used to quantify nutrient (e.g., nitrate, nitrite, ammonia, phosphate), trace metal, or pigment concentrations, or to measure the absorption spectrum of filtered seawater, especially in offshore "blue" waters where very low absorbances are observed.

CRediT authorship contribution statement

Lei Xue: Investigation, Formal analysis, Visualization, Writing – original draft, Data curation. **David J. Kieber:** Conceptualization, Supervision, Resources, Funding acquisition, Validation, Writing – review & editing.

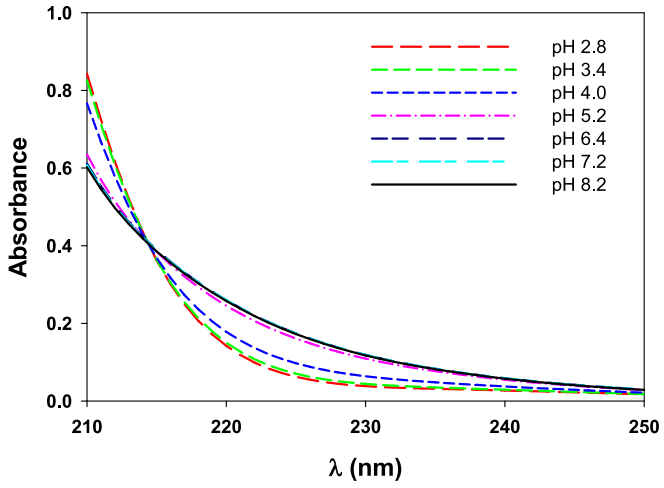

Fig 8. Absorption spectra of a 50 μM acrylate aqueous standard in phosphate buffers at different pHs determined using a model 8453 Hewlett Packard spectrophotometer with a 5 cm pathlength quartz cell. For each pH, the spectrum was referenced against the corresponding phosphate buffer solution containing no acrylate. Data used to generate this figure are presented in Table S3.

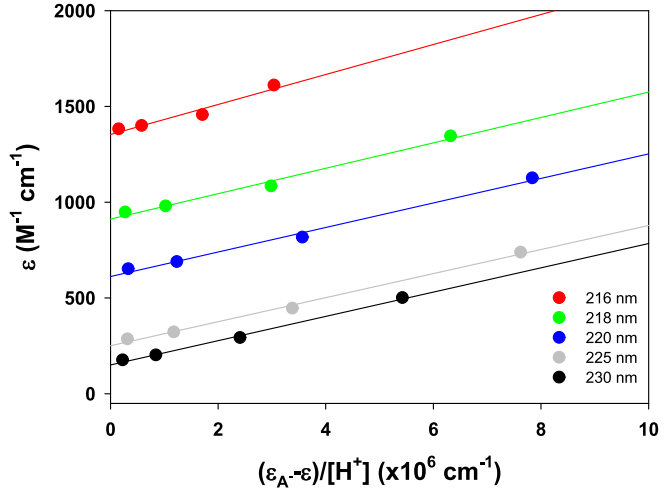

Fig 9. Molar absorptivity (ε) plotted as a function of $(\varepsilon_{A^-} - \varepsilon)/[H^+]$ (equation (4)) at 216 nm (red), 218 nm (green), 220 nm (blue), 225 nm (grey), and 230 nm (black). Each line represents the linear regression fit of the data for that wavelength. For each wavelength, ε was calculated at pH 2.8, 3.4, 4.0, and 5.2. The absorbance data used for this plot are shown in Fig. 8 and Table S3. The molar absorptivity of acrylate, ε_{A^-}, was calculated using absorbance data at pH 8.2 where the concentration of acrylic acid was negligible.

Declaration of competing interest

The authors declare that they have no known competing financial interests or personal relationships that could have appeared to influence the work reported in this paper.

Data availability

Data will be made available on request.

Acknowledgments

We thank the captain and crew of the R/V Endeavor for logistical support with the collection of a Sargasso Sea water sample during 2016 EN 589 research cruise. This study was supported by an NSF Chemical Oceanography award OCE-1756907 to DJK.

Appendix A. Supplementary data

Supplementary data to this article can be found online at https://doi.org/10.1016/j.jphotochem.2023.115371.

References

[1] Acrylic acid, Environmental Health Criteria 191 for World Health Organization, Geneva. https://inchem.org/documents/ehc/ehc/ehc191.htm, 1997.
[2] S. T. Yang, H. J. Huang, A. Tay, W. Qin, L. de Guzman, E. C. San Nicolas, Extractive fermentation for the production of carboxylic acids, in: S. T. Yang (Eds.), Bioprocessing for Value-Added Products from Renewable Resources, Elsevier, 2007, pp. 421–446.
[3] H. Danner, M. Ürmös, M. Gartner, R. Braun, Biotechnological production of acrylic acid from biomass, Appl. Biochem. Biotech. 70 (1998) 887–894, https://doi.org/10.1007/BF02920199.
[4] C.A. Staples, S.R. Murphy, J.E. McLaughlin, H.W. Leung, T.C. Cascieri, C.H. Farr, Determination of selected fate and aquatic toxicity characteristics of acrylic acid and a series of acrylic esters, Chemosphere 40 (2000) 29–38, https://doi.org/10.1016/s0045-6535(99)00228-3.
[5] J.M. Sieburth, Acrylic acid, an "antibiotic" principle in *Phaeocystis* blooms in Antarctic waters, Science 132 (1960) 676–677, https://doi.org/10.1126/science.132.3428.676.
[6] K.W. Glombitza, Antimicrobial contents in algae: 2. Presence of Acrylic Acid in Different Sea Algae, Planta Med. 18 (1970) 210–221, https://doi.org/10.1055/s-0028-1099768.
[7] D.J.B. Noordkamp, M. Schotten, W.W.C. Gieskes, L.J. Forney, J.C. Gottschal, M. van Rijssel, High acrylate concentrations in the mucus of *Phaeocystis globosa* colonies, Aquat. Microb. Ecol. 16 (1998) 45–52, https://doi.org/10.3354/ame016045.
[8] D.J.B. Noordkamp, W.W.C. Gieskes, J.C. Gottschal, L.J. Forney, M. van Rijssel, Acrylate in *Phaeocystis* colonies does not affect the surrounding bacteria, J. Sea Res. 43 (2000) 287–296, https://doi.org/10.1016/S1385-1101(00)00021-6.
[9] C. Evans, S.V. Kadner, L.J. Darroch, W.H. Wilson, P.S. Liss, G. Malin, The relative significance of viral lysis and microzooplankton grazing as pathways of dimethylsulfoniopropionate (DMSP) cleavage: An Emiliania huxleyi culture study, Limnol. Oceanogr. 52 (2007) 1036–2045, https://doi.org/10.4319/lo.2007.52.3.1036.
[10] J.D. Kinsey, D.J. Kieber, P.J. Neale, Effects of iron limitation and UV radiation on *Phaeocystis antarctica* growth and DMSP, DMSO, and acrylate concentrations, Environ. Chem. 13 (2016) 195–211, https://doi.org/10.1071/EN14275_AC.
[11] D.M. Tapiolas, C.A. Motti, P. Holloway, S.G. Boyle, High levels of acrylate in the Great Barrier Reef coral *Acropora millepora*, Coral Reefs 29 (2010) 621–625, https://doi.org/10.1007/s00338-010-0608-3.
[12] D.M. Tapiolas, J.-B. Raina, A. Lutz, B.L. Willis, C.A. Motti, Direct measurement of dimethylsulfoniopropionate (DMSP) in reef-building corals using quantitative nuclear magnetic resonance (qNMR) spectroscopy, J. Exp. Mar. Biol. Ecol. 443 (2013) 85–89, https://doi.org/10.1016/j.jembe.2013.02.037.
[13] J.-B. Raina, D.M. Tapiolas, S. Forêt, A. Lutz, D. Abrego, J. Ceh, F.O. Seneca, P. L. Clode, D.G. Bourne, B.L. Willis, C.A. Motti, DMSP biosynthesis by an animal and its role in coral thermal stress response, Nature 502 (2013) 677–680, https://doi.org/10.1038/nature12677.
[14] K. Shimokawa, Z. Kasai, Ethylene formation from acrylic acid by a banana pulp extract, Agr. Biol. Chem. 34 (1970) 1646–1651, https://doi.org/10.1080/00021369.1970.10859822.
[15] R.K. Brown, T.A. McMeekin, C. Balis, Effect of some unicellular algae on *Escherichia coli* populations in sea water and oysters, J. Appl. Bacteriol. 43 (1977) 129–136, https://doi.org/10.1111/j.1365-2672.1977.tb00731.x.
[16] M. Kodama, T. Ogata, Acrylic acid, as an antibacterial substance in scallop, Bull. Jpn. Soc. Sci. Fish. 49 (1983) 1103–1107, https://doi.org/10.2331/SUISAN.49.1103.
[17] J.H. Ansede, P.J. Pellechia, D.C. Yoch, Metabolism of acrylate to *β*-hydroxypropionate and its role in dimethylsulfoniopropionate lyase induction by a salt marsh sediment bacterium, *Alcaligenes faecalis* M3A, Appl. Environ. Microbiol. 65 (1999) 5075–5081, https://doi.org/10.1128/AEM.65.11.5075-5081.1999.
[18] J.D. Todd, A.R.J. Curson, N. Nikolaidou-Katsaraidou, C.A. Brearley, N. J. Watmough, Y. Chan, P.C.B. Page, L. Sun, A.W.B. Johnston, Molecular dissection of bacterial acrylate catabolism – unexpected links with dimethylsulfoniopropionate catabolism and dimethylsulfide production, Environ. Microbiol. 12 (2010) 327–343, https://doi.org/10.1111/j.1462-2920.2009.02071.x.
[19] A.R.J. Curson, O.J. Burns, S. Voget, R. Daniel, J.D. Todd, K. McInnis, M. Wexler, A. W.B. Johnston, Screening of metagenomic and genomic libraries reveals three classes of bacterial enzymes that overcome the toxicity of acrylate, PLoS One 9 (2014) e97660.
[20] P. Wang, H.Y. Cao, X.L. Chen, C.Y. Li, P.Y. Li, X.Y. Zhang, Q.L. Qin, J.D. Todd, Y. Z. Zhang, Mechanistic insight into acrylate metabolism and detoxification in marine dimethylsulfoniopropionate-catabolizing bacteria, Mol. Microbiol. 105 (2017) 674–688, https://doi.org/10.1111/mmi.13727.
[21] R.C. Noble, J.W. Czerkawski, A gas-chromatographic method for the determination of low concentrations of acrylic acid in mixtures of C2 and C5 fatty acids in biological materials, Analyst 98 (1973) 122–125, https://doi.org/10.1039/AN9739800122.
[22] J.M. Sieburth, Antibiotic properties of acrylic acid, a factor in the gastrointestinal antibiosis of polar marine animals, J. Bacteriol. 82 (1961) 72–79, https://doi.org/10.1128/JB.82.1.72-79.1961.
[23] J.W.H. Dacey, G.M. King, P.S. Lobel, Herbivory by reef fishes and the production of dimethylsulfide and acrylic acid, Mar. Ecol. Prog. Ser. 112 (1994) 67–74, https://doi.org/10.3354/meps112067.
[24] P. Schmitt-Kopplin, G. Liger-Belair, B.P. Koch, R. Flerus, G. Kattner, M. Harir, B. Kanawati, M. Lucio, D. Tziotis, N. Hertkorn, I. Gebefügi, Dissolved organic matter in sea spray: A transfer study from marine surface water to aerosols, Biogeosciences 9 (2012) 1571–1582, https://doi.org/10.5194/bg-9-1571-2012.
[25] H. Yang, A.R. McTaggart, A.T. Davidson, H. Burton, Measurement of acrylic acid and dimethylsulfide in Antarctic coastal water during a summer bloom of *Phaeocystis pouchetii*, Proc. NIPR Symp. Polar Biol. 7 (1994) 43–52.
[26] J.A.E. Gibson, K.M. Swadling, H.R. Burton, Acrylate and dimethylsulfoniopropionate (DMSP) concentrations during an Antarctic phytoplankton bloom, in: R.P. Kiene, P.T. Visscher, M.D. Keller, G.O. Kirst (Eds.), Biological and Environmental Chemistry of DMSP and Related Sulfonium Compounds, Plenum Press, New York, 1996, pp. 213–222.
[27] I.M.B. Tyssebotn, J.D. Kinsey, D.J. Kieber, R.P. Kiene, A.N. Rellinger, J. Motard-Côté, Concentrations, biological uptake, and respiration of dissolved acrylate and dimethylsulfoxide in the northern Gulf of Mexico, Limnol. Oceanogr. 62 (2017) 1198–1218, https://doi.org/10.1002/lno.10495.
[28] L. Xue, D.J. Kieber, M. Masdeu-Navarro, M. Cabrera-Brufau, P. Rodríguez-Ros, S. G. Gardner, C. Marrasé, R. Simó, Concentrations, sources, and biological consumption of acrylate and DMSP in the tropical Pacific and coral reef ecosystem in Mo'orea, French Polynesia, Front. Mar. Sci. 9 (2022), 911522, https://doi.org/10.3389/fmars.2022.911522.
[29] A.R.J. Curson, J.D. Todd, M.J. Sullivan, A.W. Johnston, Catabolism of dimethylsulphoniopropionate: microorganisms, enzymes and genes, Nat. Rev. Microbiol. 9 (2011) 849–859, https://doi.org/10.1038/nrmicro2653.
[30] G.L. Cantoni, D.G. Anderson, E. Rosenthal, Enzymatic cleavage of dimethylpropiothetin by *Polysiphonia lanosa*, J. Biol. Chem. 222 (1956) 171–177, https://doi.org/10.1016/S0021-9258(19)50782-7.
[31] K.W. Glombitza, Antibiotics from algae, in: H.A. Hoppe, T. Levring, J. Tanaka (Eds.), Marine Algae in Pharmaceutical Science, Walter de Gruyter, Berlin, New York, 1979, pp. 303–307.
[32] D.M. Slezak, S. Puskaric, G.J. Herndl, Potential role of acrylic acid in bacterioplankton communities in the sea, Mar. Ecol. Prog. Ser. 105 (1994) 191–197, https://doi.org/10.3354/meps105191.
[33] G.V. Wolfe, M. Steinke, G.O. Kirst, Grazing-activated chemical defense in a unicellular marine alga, Nature 387 (1997) 894–897, https://doi.org/10.1038/43168.
[34] W. Sunda, D.J. Kieber, R.P. Kiene, S. Huntsman, An antioxidant function for DMSP and DMS in marine algae, Nature 418 (2002) 317–320, https://doi.org/10.1038/nature00851.
[35] J. Stefels, Physiological aspects of the production and conversion of DMSP in marine algae and higher plants, J. Sea Res. 43 (2000) 183–197, https://doi.org/10.1016/S1385-1101(00)00030-7.
[36] K.M. Ledyard, E.F. DeLong, J.W.H. Dacey, Characterization of a DMSP-degrading bacterial isolate from the Sargasso Sea, Arch. Microbiol. 160 (1993) 312–318, https://doi.org/10.1007/BF00292083.
[37] J.M. Gonzalez, R.P. Kiene, M.A. Moran, Transformation of sulfur compounds by an abundant lineage of marine bacteria in the α-subclass of the class *Proteobacteria*, Appl. Environ. Microbiol. 65 (1999) 3810–3819, https://doi.org/10.1128/AEM.65.9.3810-3819.1999.
[38] J.-B. Raina, D.M. Tapiolas, B.L. Willis, D.G. Bourne, Coral-associated bacteria and their role in the biogeochemical cycling of sulfur, Appl. Environ. Microbiol. 75 (2009) 3492–3501, https://doi.org/10.1128/AEM.02567-08.
[39] M. Garren, K. Son, J.-B. Raina, R. Rusconi, F. Menolascina, O. H. Shapiro, J. Tout, D. G. Bourne, A bacterial pathogen uses dimethylsulfoniopropionate as a cue to target heat stressed corals, ISME J. 8 (2014) 999–1007. doi:10.1038/ismej.2013.210.
[40] J.H. Ansede, P.J. Pellechia, D.C. Yoch, Nuclear magnetic resonance analysis of [1-13C]dimethylsulfoniopropionate (DMSP) and [1-13C]acrylate metabolism by a DMSP lyase-producing marine isolate of the α-subclass of proteobacteria, Appl. Environ. Microbiol. 67 (2001) 3134–3139, https://doi.org/10.1128/AEM.67.7.3134-3139.2001.
[41] M. Fujita, Y. Iizuka, A. Miyake, Thermal and kinetic analyses on Michael addition reaction of acrylic acid, J. Therm. Anal. Calorim. 128 (2017) 1227–1233, https://doi.org/10.1007/s10973-016-5985-6.
[42] L.B. Levy, J.D. Penrod, The anatomy of an acrylic acid runaway polymerization, Plant/Oper Prog. 8 (1989) 105–108, https://doi.org/10.1002/prsb.720080216.
[43] D. Shemesh, R.B. Gerber, Molecular dynamics of photoinduced reactions of acrylic acid: Products, mechanisms, and comparison with experiment, J. Phys. Chem. Lett. 9 (2018) 527–533, https://doi.org/10.1021/acs.jpclett.7b03015.

[44] R.N. Rosenfeld, B.R. Weiner, Photofragmentation of acrylic acid and methacrylic acid in the gas phase, J. Am. Chem. Soc. 105 (1983) 6233–6236, https://doi.org/10.1021/ja00358a007.
[45] D. Budac, P. Wan, Photodecarboxylation: Mechanism and synthetic utility, J. Photochem. Photobiol. A Chem. 67 (1992) 135–166, https://doi.org/10.1016/1010-6030(92)85224-I.
[46] W.D. Closson, S.F. Brady, P.J. Orenski, The electronic absorption spectra of carboxylate derivatives. III. Effects of solvent and structure on the absorption spectra of α, β-unsaturated esters, J. Org. Chem. 30 (1965) 4026–4031, https://doi.org/10.1021/jo01023a009.
[47] V. Lüthy, Absorption spectra in the ultraviolet from unsaturated links: Vapor spectra from acrolein, crotonaldehyde and glyoxal, Z. Phys. Chem. 107 (1923) 285–304.
[48] H. Morita, K. Fuke, S. Nagakura, Electronic structure and spectra of acrylic acid in the vapor and condensed phases, B. Chem. Soc. Jpn. 49 (1976) 922–928, https://doi.org/10.1246/bcsj.49.922.
[49] J.W.H. Dacey, N.V. Blough, Hydroxide decomposition of dimethylsulfoniopropionate to form dimethylsulfide, Geophys. Res. Lett. 14 (1987) 1246–1249, https://doi.org/10.1029/GL014i012p01246.
[50] C.M. Cartisano, R. Del Vecchio, N.V. Blough, A calibration/validation protocol for long/multi-pathlength capillary waveguide spectrometers, Limnol. Oceanogr. Methods 16 (2018) 773–786, https://doi.org/10.1002/lom3.10282.
[51] N.B. Nelson, D.A. Siegel, C.A. Carlson, C.M. Swan, W.M. Smethie, S. Khatiwala, Hydrography of chromophoric dissolved organic matter in the North Atlantic, Deep-Sea Res. I (54) (2007) 710–731, https://doi.org/10.1016/j.dsr.2007.02.006.
[52] M. Fischer, P. Warneck, The dissociation constant of pyruvic acid: Determination by spectrophotometric measurements, Phys. Chem. 95 (1991) 523–527, https://doi.org/10.1002/bbpc.19910950414.
[53] S. Nagakura, K. Kaya, H. Tsubomura, Vacuum ultraviolet absorption spectra and electronic structures of formic acid, acetic acid and ethyl acetate, J. Mol. Spectrosc. 13 (1964) 1–8, https://doi.org/10.1016/0022-2852(64)90049-9.
[54] L. Xue, D.J. Kieber, Photochemical production and photolysis of acrylate in seawater, Environ. Sci. Technol. 55 (2021) 7135–7144, https://doi.org/10.1021/acs.est.1c00327.
[55] J. Calvert, J. Pitts, Photochemistry, John Wiley & Sons, Inc., New York, 1966.
[56] U. Weiss, H. Ziffer, Cotton effects of α, β-unsaturated carboxylic acids, J. Org. Chem. 5 (1963) 1248–1251, https://doi.org/10.1021/jo01040a021.
[57] W.D. Closson, S.F. Brady, E.M. Kosower, P.C. Huang, The n → π * transition of α, β-unsaturated esters, J. Org. Chem. 28 (1963) 1161–1162, https://doi.org/10.1021/jo01039a066.
[58] C. Reichardt, T. Welton, Solvent effects on the absorption spectra of organic compounds, in: C. Reichardt, T. Welton (Eds.), Solvents and Solvent Effects in Organic Chemistry, 4th ed., Wiley-VCH Verlag GmbH & Co. KGaA, Weinheim, Germany, 2010, pp. 359–424.
[59] I.W. Sizer, A.C. Peacock, The ultraviolet absorption of serum albumin and of its constituent amino acids as a function of pH, J. Biol. Chem. 171 (1947) 767–777, https://doi.org/10.1016/S0021-9258(17)41087-8.
[60] N. Kretchmer, R. Taylor, Effect of pH on the far ultraviolet absorption of tyrosine, Am. Chem. Soc. 72 (1950) 3291–3292, https://doi.org/10.1021/ja01163a520.
[61] D.B. Wetlaufer, Ultraviolet spectra of proteins and amino acids, Adv. Protein Chem. 17 (1963) 303–390, https://doi.org/10.1016/S0065-3233(08)60056-X.
[62] M. Falk, J.A. Walter, P.W. Wiseman, Ultraviolet spectrum of domoic acid, Can. J. Chem. 67 (1989) 1421–1425, https://doi.org/10.1139/v89-218.
[63] M. Szyper, P. Zuman, Electronic absorption of carboxylic acids and their anions, Analytica Chimica Acta. 85 (1976) 357–373, https://doi.org/10.1016/S0003-2670(01)84702-4.
[64] J.A. Dean, Lange's Handbook of Chemistry, 15th ed., McGraw-Hill Inc., New York, 1999.